Nebulin stiffens the thin filament and augments cross-bridge interaction in skeletal muscle

Balázs Kiss[a], Eun-Jeong Lee[a], Weikang Ma[b], Frank W. Li[a], Paola Tonino[a], Srboljub M. Mijailovich[b], Thomas C. Irving[b], and Henk L. Granzier[a,1]

[a]Department of Cellular and Molecular Medicine, University of Arizona, Tucson, AZ 85721; and [b]Department of Biology, Illinois Institute of Technology, Chicago, IL 60616

Edited by Christine E. Seidman, Howard Hughes Medical Institute and Brigham and Women's Hospital, and Harvard Medical School, Boston, MA, and approved August 30, 2018 (received for review March 19, 2018)

Nebulin is a giant sarcomeric protein that spans along the actin filament in skeletal muscle, from the Z-disk to near the thin filament pointed end. Mutations in nebulin cause muscle weakness in nemaline myopathy patients, suggesting that nebulin plays important roles in force generation, yet little is known about nebulin's influence on thin filament structure and function. Here, we used small-angle X-ray diffraction and compared intact muscle deficient in nebulin (using a conditional nebulin-knockout, Neb cKO) with control (Ctrl) muscle. When muscles were activated, the spacing of the actin subunit repeat (27 Å) increased in both genotypes; when converted to thin filament stiffness, the obtained value was 30 pN/nm in Ctrl muscle and 10 pN/nm in Neb cKO muscle; that is, the thin filament was approximately threefold stiffer when nebulin was present. In contrast, the thick filament stiffness was not different between the genotypes. A significantly shorter left-handed (59 Å) thin filament helical pitch was found in passive and contracting Neb cKO muscles, as well as impaired tropomyosin and troponin movement. Additionally, a reduced myosin mass transfer toward the thin filament in contracting Neb cKO muscle was found, suggesting reduced cross-bridge interaction. We conclude that nebulin is critically important for physiological force levels, as it greatly stiffens the skeletal muscle thin filament and contributes to thin filament activation and cross-bridge recruitment.

X-ray diffraction | skeletal myopathy | muscle biology | physiology

Nebulin is a giant ∼800 kDa sarcomeric protein whose functions have remained nebulous (1–3). Previous studies have shown that nebulin extends along the thin filament, with its C terminus near the barbed end of the thin filament (at the Z-disk) and its N terminus near the pointed end (4–6). Nebulin has been shown to act as a length-regulating template that determines thin filament length in skeletal muscle (6, 7). The protein contains 185 tandem copies of an ∼35-aa domain (with a conserved SDxxYK motif) referred to as a simple nebulin repeat (1, 3). It has been postulated that each simple repeat interacts directly with one actin subunit along the thin filament (8) and that nebulin is orientated along the long-pitch helices of actin (1, 9). Most of the simple repeats are organized in seven-module super repeats (with a conserved WLKGIGW motif) that correspond to the arrangement of troponin and tropomyosin on the thin filament. Mutations in nebulin are the main cause of nemaline myopathy, a progressive skeletal muscle disease characterized by a large deficit in force (10). Mechanical studies on muscle fibers deficient in nebulin, from both mice and patients (11), show that nebulin deficiency results in a large force reduction (11–13). However, the detailed mechanisms of how nebulin deficiency causes a force deficit remain to be established.

X-ray diffraction is an ideal technique to characterize myofilaments in intact muscle (14). Although no nebulin-based reflections can be detected in skeletal muscle due to the slender nebulin backbone, we addressed nebulin's role in muscle by investigating myofilament-based X-ray–derived parameters in intact muscle of a conditional nebulin KO (Neb cKO) model. Small spacing changes in the higher-order meridional reflections in response to muscle activation denote the axial extensibility of actin and myosin subunits and are therefore sensitive indicators of myofilament ultrastructure (15–18). Additionally, whereas higher-order actin layer lines represent the geometry of the thin filament helix (19), its lower-order layer lines reflect the movement of the regulatory proteins on the thin filament (20, 21). We provide evidence that nebulin stiffens the thin filament by acting on its actin subunits, fine-adjusts its helix, and is required for optimal tropomyosin/troponin movement on the thin filament. Furthermore, by characterizing the equatorial reflections (22) and higher-order myosin layer lines that are indicative of cross-bridge behavior (23), we show that upon activation, nebulin promotes recruitment of myosin heads toward the thin filament. Thus, nebulin is critical for physiological force levels in skeletal muscle because it stiffens the thin filament, promotes thin filament activation, and enhances cross-bridge recruitment.

Results

Soleus muscles from Ctrl and Neb cKO mice were electrically stimulated to achieve a maximal tetanic contraction, and X-ray diffraction images were recorded during the passive state immediately before activation and during force development (Fig. 1 *A* and *B*). Blebbistatin was used in some experiments to lower tetanic force and study the force dependence of the X-ray reflections of interest. We extensively analyzed the thin filament-specific

Significance

Nebulin is a giant actin-binding protein in skeletal muscle which localizes along most of the length of the thin filament. Genetic alterations or reduction in the expression level of nebulin are accompanied by dramatic loss in muscle force, resulting in muscle weakness and severe skeletal muscle myopathy. Using an inducible and tissue-specific nebulin-knockout mouse model in which nebulin is not expressed in skeletal muscle, we investigated the ultrastructure of thin filaments in passive and contracting muscle under physiological conditions using X-ray diffraction. Thin filaments were found to be threefold less stiff in nebulin-knockout muscle, and thin filament regulatory protein and cross-bridge behavior was impaired. Nebulin stiffens the thin filaments and is responsible for generating physiological levels of force.

Author contributions: B.K., E.-J.L., T.C.I., and H.L.G. designed research; B.K., E.-J.L., W.M., F.W.L., P.T., T.C.I., and H.L.G. performed research; B.K., W.M., S.M.M., T.C.I., and H.L.G. contributed new reagents/analytic tools; B.K., E.-J.L., W.M., S.M.M., T.C.I., and H.L.G. analyzed data; and B.K. and H.L.G. wrote the paper.

The authors declare no conflict of interest.

This article is a PNAS Direct Submission.

[1]To whom correspondence should be addressed. Email: granzier@email.arizona.edu.

This article contains supporting information online at www.pnas.org/lookup/suppl/doi:10.1073/pnas.1804726115/-/DCSupplemental.

Published online September 24, 2018.

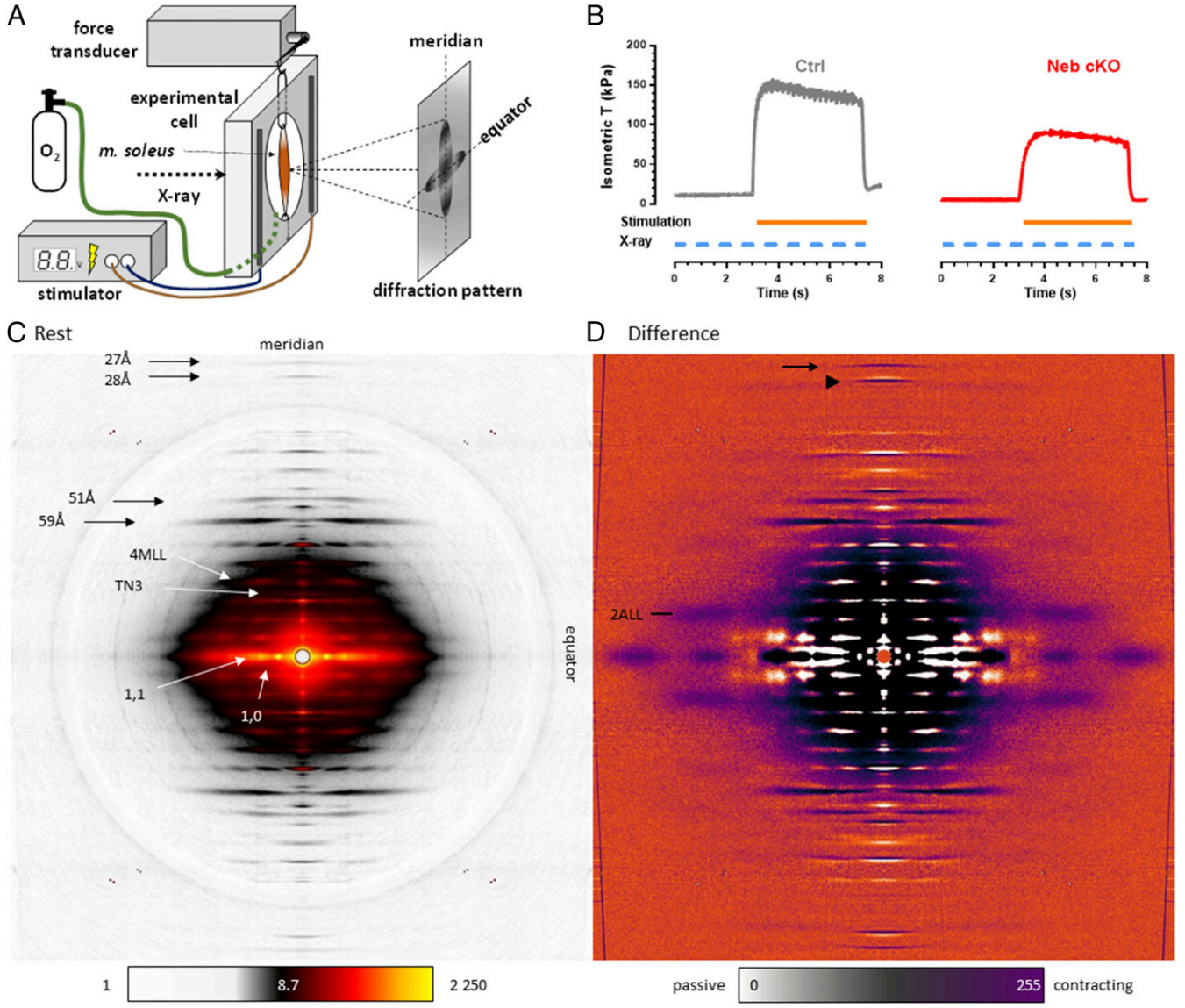

Fig. 1. X-ray diffraction of intact mouse soleus muscle (m. soleus). (*A*) Experimental setup showing the alignment of the muscle. (*B*) Isometric activation of Ctrl and Neb cKO soleus showing reduced active tension in Neb cKO. X-ray diffraction data were collected during resting and tetanic phases. (*C*) X-ray diffraction image of m. soleus at rest. The diffraction peaks of interest are indicated. Nonlinear scale bar indicates intensity. (*D*) Difference X-ray diffraction (contracting minus resting) from the same muscle. Purple areas represent high intensity during isometric contraction, whereas white pixels indicate high intensity at rest. Arrow indicates 27 Å reflection; arrowhead indicates 28 Å reflection; and linear scale bar indicates intensity difference.

27 Å meridional reflection (actin subunit spacing) (15, 16, 18) and the 51 Å and 59 Å layer line reflections (short- and long-pitch helix periodicity of the actin filament, respectively) (19). Furthermore, to follow the structural changes affecting myosin, myofilament lattice, and cross-bridge behavior in Ctrl and Neb cKO muscles, the 28 Å meridional reflection (thick filament backbone) (17, 18), the 1,0 and 1,1 equatorials (22, 23) and the fourth myosin layer line (4MLL) were also studied (Fig. 1*C*). The 4MLL was chosen for analysis since it lacks lattice sampling and does not overlap with actin-based layer lines (24). The small spacing changes of the higher-order 27 Å and 28 Å meridionals (Fig. 1*D*) could be accurately revealed on high-resolution meridional plot profiles (*SI Appendix*, Fig. S1). The far off-meridional part of the second actin layer line (2ALL) (tropomyosin) reflection was detectable during activation and was subsequently analyzed on difference images (Fig. 1*D*). The third-order troponin (TN3) meridional was followed to assess changes in troponin spacing (Fig. 1*C*).

Nebulin Stiffens the Thin Filament. The percent spacing change of the 27 Å meridional reflection between passive and tetanic plateau tension shows a linear dependence on tension in both the Ctrl and Neb cKO muscles (Fig. 2*A*). This tension dependence is consistent with earlier findings on intact frog muscle (15, 16, 18, 25), but what is striking about the present finding is that the slope of the Neb cKO curve (0.0075%/kPa) is approximately threefold larger than that of the Ctrl (0.0027%/kPa). This indicates increased actin extensibility in Neb cKO muscle. This difference is readily visible on meridional plot profiles (*SI Appendix*, Fig. S1). In contrast to the thin filament behavior, the tension dependence of the 28 Å reflection (based on the thick filament backbone) scales nonlinearly with isometric tension, and the Ctrl and Neb cKO datasets superimpose (Fig. 2*B*).

We performed time-resolved experiments and measured the absolute 27 Å and 28 Å spacings before and during the tetanic force rise. By plotting the 27 Å spacing vs. tension (*SI Appendix*, Fig. S2*B*), the previously found linear tension dependence is

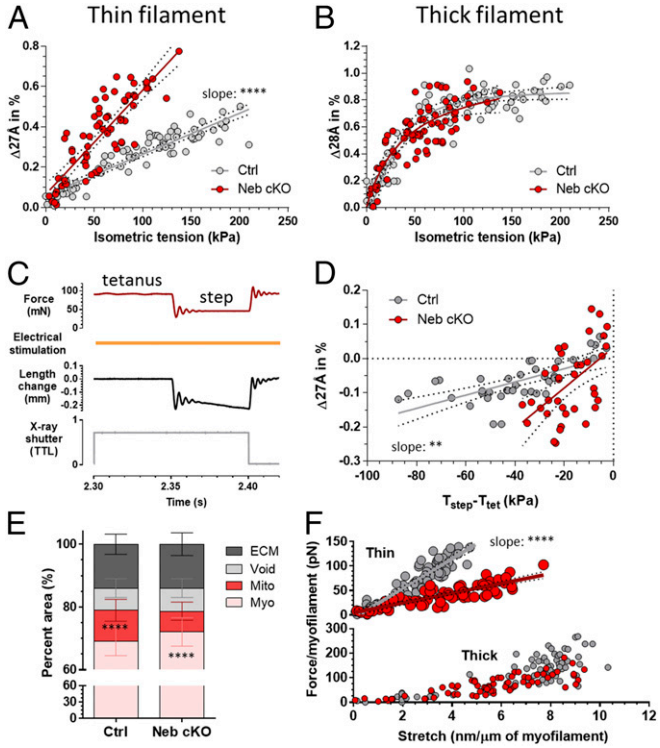

Fig. 2. Effect of nebulin on myofilament compliance. (*A*) The 27 Å relative spacing change as a function of isometric contraction. (*B*) Tension dependence of the 28 Å reflection. (*C*) Force step protocol on activated muscle. Tetanic force was reduced and held constant by controlling the muscle length. TTL, logic voltage level. (*D*) The 27 Å relative spacing change during the force step protocol in Ctrl and Neb cKO. T, tension. (*E*) Cross-sectional ultrastructural analysis of Ctrl and Neb cKO soleus showing the percent area of myofibrils (Myo), mitochondria (Mito), void regions (Void), and extracellular matrix (ECM). (*F*) Average force per single thin (*Top*) and thick (*Bottom*) filament as a function of longitudinal stretch. Stretch was calculated from the 27 Å and 28 Å relative spacing change extrapolated to a 1-μm-long thin and thick filament, respectively. $^{**}P < 0.01$; $^{****}P < 0.0001$.

revealed again: Neb cKO samples show an increased slope (5.1×10^{-5} nm/kPa in Ctrl, 12.9×10^{-5} nm/kPa in cKO). The 28 Å spacing sensitively follows the isometric tension in both genotypes (*SI Appendix*, Fig. S2*C*). The tension dependence of the 28 Å spacing is nonlinear (*SI Appendix*, Fig. S2*D*), and the Ctrl and Neb cKO data superimpose, consistent with the steady-state spacing-change dataset (Fig. 2*B*).

To address the possibility that muscle activation itself affects the 27 Å spacing and confounds our findings, muscles were exposed to sudden force reductions (step) during tetanic activation (Fig. 2*C*). Following the 27 Å spacing change as a function of the tension reduction, a linear response was found in both the Ctrl and Neb cKO (Fig. 2*D*) muscles. Both lines have significantly nonzero slopes with values (Ctrl, 0.00193%/kPa; Neb cKO, 0.00592%/kPa) that differ significantly ($P = 0.0045$). Note the approximately threefold increase in the 27 Å spacing change of the Neb cKO, consistent with the 27 Å data obtained during the tetanic force plateau.

To determine the stiffness of the thin and thick filaments, it is important to investigate how the isometric tension is distributed over the myofilaments. Hence, an ultrastructural analysis was performed on electron micrographs of Ctrl and Neb cKO soleus cross-sections, the results of which are shown in Fig. 2*E*. Interestingly, a significantly larger myofibrillar fractional area was found in Neb cKO (72.1%) compared with Ctrl (69.2%), at the expense of the mitochondrial area that was significantly reduced in Neb cKO (6.6% vs. 9.8% in Ctrl). We then calculated the force per individual myofilament in activated muscle. Briefly, the unit cell area of the myofilament lattice was calculated from the $d_{1,0}$ equatorial spacing (*SI Appendix*, Fig. S3) according to ref. 22, with the number of unit cells per muscle cross-section equaling the myofibril area divided by the unit cell area. Furthermore, the tension distribution along the thin and thick filaments was determined from their lengths and the overlap between them according to refs. 16 and 26 (for calculations, see *SI Appendix*, *Supplemental Methods*). The force obtained per thin filament (Fig. 2*F*) was found to vary linearly with stretch in both genotypes, but thin filaments of the Neb cKO muscle are significantly more extensible based on the slope of the regression line [(10.0 pN·nm^{-1}·μm^{-1}) in Neb cKO vs. 30.3 pN·nm^{-1}·μm^{-1} in Ctrl; Fig. 2*F*, *Top*]. The thick filament backbone extends linearly below 100 pN force (Fig. 2*F*, *Bottom*). No difference was found between the genotypes in their regression lines, for both the Ctrl and Neb cKO (slope, 15.2 pN·nm^{-1}·μm^{-1}). We conclude that nebulin does not affect thick filament extensibility but that it stiffens the thin filament approximately threefold.

To gain insight into how thin filament stiffness affects active force generation in skeletal muscle, we simulated a 3D sarcomere lattice with standard geometry and standard activation kinetics and cross-bridge cycling parameters, but with different thin filament stiffness (for details, see ref. 27 and *SI Appendix*, Fig. S4 *A* and *B*). Reducing the thin filament stiffness from Ctrl levels to the level of the Neb cKO resulted in greatly reduced sarcomere stiffness and speed of force development. However, at steady state, there was little effect on the maximal force and the number of active cross-bridges (*SI Appendix*, Fig. S4*C*, *Bottom*). Simulations assuming several different thin filament stiffness values show that both muscle stiffness and isometric tension are reduced with increasing thin filament compliance [the reduction was 49% in sarcomere stiffness and 1% in isometric tension, assuming 30 pN/nm (Ctrl) and 10 pN/nm (Neb cKO) thin filament stiffness, respectively (*SI Appendix*, Fig. S4*D*)]. Thus, reducing thin filament stiffness has only a small effect on maximal tetanic force but a large effect on muscle stiffness.

Nebulin Modulates the Thin Filament Helix and Tropomyosin and Troponin Behavior. To assess the effect of the actin subunit extensibility on the actin filament structure, we studied the 51 Å and 59 Å actin layer lines (19, 25). No significant difference was revealed between the genotypes regarding the 51 Å spacing during rest or during tetanic activation (Fig. 3*A*, *Top* and *Bottom*). Strikingly, the 59 Å spacing was significantly decreased in resting Neb cKO soleus compared with Ctrl, and the shorter 59 Å spacing in Neb cKO was maintained during tetanic force development (Fig. 3*B*, *Top* and *Bottom*, also see *SI Appendix*, Fig. S5).

To address whether the thin filament regulatory proteins tropomyosin and troponin are influenced by nebulin, we studied the off-meridional 2ALL (tropomyosin) (21) and meridional TN3 (troponin) (28) reflections (for their locations see Fig. 1 *C* and *D*). The 2ALL reflection was visualized in difference images obtained by subtracting the contracting pattern from the resting one (Fig. 4*A* shows an example plot profile). Significantly less-intense and broader 2ALL peaks were found in Neb cKO muscle, indicating impaired tropomyosin movement (Fig. 4 *A* and *B*). The intensity of the TN3 reflection was significantly reduced in resting Neb cKO muscle (Fig. 4*C*), indicating that troponin (mass) distribution is altered in passive muscles deficient in nebulin. This anomalous troponin configuration was maintained in activated muscle: Whereas TN3 intensity increased in Ctrl with contraction, a significant decrease was found in Neb cKO (Fig. 4*D*).

Nebulin Recruits Actomyosin Cross-Bridges. To evaluate whether the presence of nebulin affects cross-bridge behavior, we determined the intensity ratios of the 1,1 and 1,0 equatorial reflections (22, 23). Compared with Ctrl muscle, Neb cKO muscle had a significantly lower $I_{1,1}/I_{1,0}$ ratio in both passive (Fig. 5*A*) and contracting muscles (Fig. 5*B*). We also studied the 4MLL (Fig. 1*C*). The intensity distribution on the 4MLL reflects the highly ordered helical arrangement of myosin heads around the

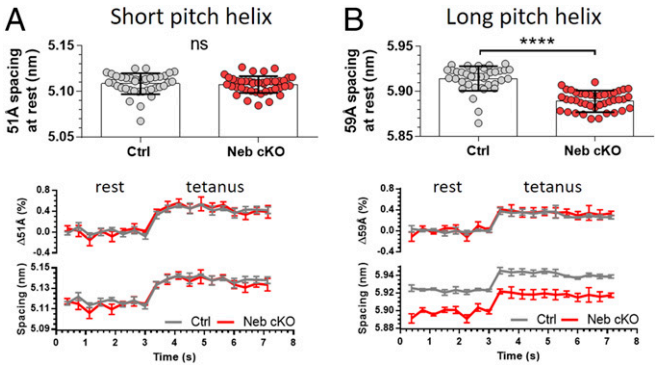

Fig. 3. Effect of nebulin on thin filament helix and cross-bridge behavior. The 51 Å (*A*) and 59 Å (*B*) spacing in Ctrl and Neb cKO muscles. (*A* and *B*, *Top*) Values at rest. (*A* and *B*, *Bottom*) Graphs during the rest-to-tetanus transition, with the *Upper* graph demonstrating the relative spacing change normalized to the average spacing at rest. For each data point, 25 consecutive diffraction frames were averaged, resulting in 0.375 s time resolution. For each genotype, five time-resolved spacing traces were averaged. ns, not significant ($P \geq 0.05$); ****$P < 0.0001$.

thick filament backbone and is strongest in relaxed muscle where myosin head "crowns" decorate the thick filament at fixed axial intervals (29). At rest, we found no difference in the 4MLL intensities between the genotypes, indicating that the majority of the myosin heads are helically ordered around the thick filament and that the proportion of the ordered heads is about the same in both genotypes (Fig. 5*C*, Resting). (The discrepancy between the equatorial intensity analysis and the 4MLL is discussed below.) Furthermore, the distance to the first maximum on the 4MLL was unchanged in Ctrl and Neb cKO muscles (13.06 ± 0.56 and 12.95 ± 0.40 nm, respectively, $P = 0.57$), indicating no difference in the resting distributions of myosin heads. The 4MLL intensity was reduced during tetanic contraction due to the loss of order when myosin heads interact with the thin filament, but the reduction was much less in Neb cKO (Fig. 5*C*, Tetanized). As a result, the ratio of tetanic to the passive 4MLL intensities was significantly higher in Neb cKO (Fig. 5*D*). This finding indicates that in activated muscle, the proportion of the ordered myosin heads that remains around the thick filament backbone is significantly higher in the absence of nebulin. Hence, the presence of nebulin promotes cross-bridge recruitment.

Discussion

The present X-ray diffraction study shows that nebulin stiffens the thin filament and that this increases the stiffness of activated skeletal muscle and the speed of force development. Additionally, nebulin alters the behavior of the regulatory proteins tropomyosin and troponin and enhances the recruitment of cross-bridges toward the thin filament. It is likely that through these effects on thin filament structure, nebulin contributes to the high calcium sensitivity and high maximal active force levels that characterize skeletal muscle.

The actin subunit spacing (27 Å reflection) scales linearly with active tension in both Ctrl and Neb cKO muscles over a wide tension range. This linear relation was found both during the isometric tetanus plateau (Fig. 2*A*) and during step-force changes (Fig. 2*D*), suggesting that it solely reflects the passive material property of the thin filament, and not an activation process [unlike the thick filament extensibility (15)]. Actin subunit strain is expected to be different among thin filaments of variable length in Neb cKO muscle (30). This would manifest in the broadening of their tetanic 27 Å peaks (as can be seen in *SI Appendix*, Fig. S1), although it is not expected to alter the position of the peak centroid that still correctly represents the average behavior of the actin subunits. Extrapolation of the 27 Å spacing change to a 1-μm-long thin filament with its plot against the tetanic force per thin filament shows that the actin subunits behave as linearly elastic spring elements (Fig. 2*F*), with a spring constant of 30 $pN{\cdot}nm^{-1}{\cdot}\mu m^{-1}$ for Ctrl and 10 $pN{\cdot}nm^{-1}{\cdot}\mu m^{-1}$ for Neb cKO thin filaments. These values are less than the 65 $pN{\cdot}nm^{-1}{\cdot}\mu m^{-1}$ measured in vitro on reconstituted and tropomyosin-decorated single actin filaments (31). However, these experiments on single filaments used phalloidin to visualize actin and this is likely to have stiffened the thin filaments, as suggested by studies on thin filaments undergoing 2D Brownian movement (32). Thus, the in vitro stiffness value is likely to be increased due to the use of phalloidin. Here, we report a label-free in vivo stiffness value of mammalian skeletal muscle thin filaments with and without nebulin; our results unequivocally reveal that nebulin stiffens the thin filament. A small amount of residual nebulin (9.4% of Ctrl levels) was still expressed in the Neb cKO soleus muscle (*SI Appendix*, Fig. S6). It is likely that this residual nebulin is homogeneously distributed among the sarcomeres, as supported by protein expression studies and our X-ray diffraction data showing that wider but still single and symmetrical 27 Å (*SI Appendix*, Fig. S1) and 2ALL intensity profiles were found in Neb cKO (Fig. 4*A*). Assuming that the small amount of residual nebulin is fully and evenly incorporated into the thin filaments, the stiffening effect of the residual nebulin would cause a slight underestimation of extensibility of thin filaments completely devoid of nebulin. Extrapolation from the stiffness of Ctrl (100% nebulin) and Neb cKO (9.4% nebulin) would predict 7.9 $pN{\cdot}nm^{-1}{\cdot}\mu m^{-1}$ thin filament stiffness in the full absence of nebulin. Simulations using a 3D stochastic model of cross-bridge interaction in the sarcomere lattice (27) revealed that the increased thin filament stiffness speeds force development (*SI Appendix*, Fig. S4), which is likely functionally important in skeletal muscle that operates at fast time scales.

The thin filament contributes to the series extensibility of the cross-bridge and thereby affects the force levels that cross-bridges generate (18). However, our simulation revealed that the reduced thin filament stiffness in Neb cKO muscle reduces isometric force by only ∼1% (*SI Appendix*, Fig. S4). This small reduction clearly cannot explain the ∼50% force deficits measured in both nebulin-deficient intact muscle (*SI Appendix*, Fig. S7) and calcium-activated skinned fibers (12). What then might explain these large force deficits? It is unlikely that a reduced myofibrillar fractional area (e.g., if myofibrils were to be less densely packed) plays a major role, as our cross-sectional analysis revealed a small but significant increase in the myofibrillar fractional area (at the expense of the mitochondrial area, which is reduced) (Fig. 2*E*). Additionally, the number of fibers per cross-section in Neb cKO

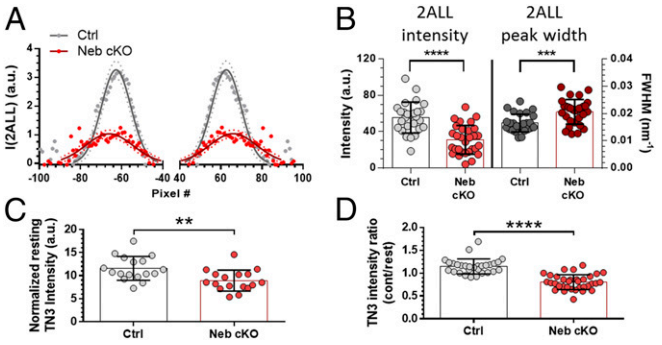

Fig. 4. Tropomyosin and troponin movement on the thin filament. (*A*) Off-meridional tracing of the 2ALL of Ctrl and Neb cKO soleus. Continuous line indicates Gaussian fit; dotted lines indicate 95% CI of the Gaussian fit. I, intensity. (*B*) Integral intensity and width distribution of the 2ALL peaks of Ctrl and Neb cKO. FWHM, full width at half maximum, in reciprocal space. (*C*) Resting intensity of the TN3 meridional reflection in Ctrl and Neb cKO muscles normalized to the total volume of their thin filaments. (*D*) Relative intensity change of TN3 calculated as intensity of TN3 with contraction (cont) divided by intensity of TN3 at rest. **$P < 0.01$; ***$P < 0.001$; ****$P < 0.0001$.

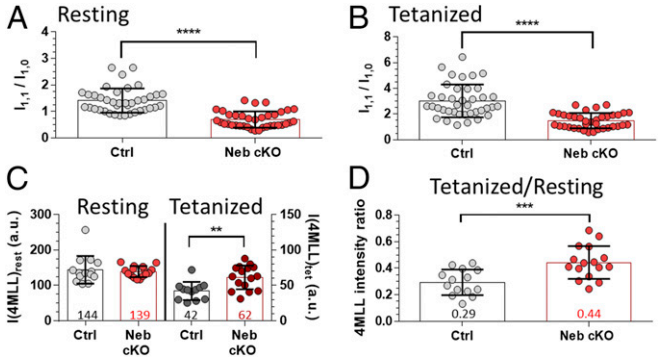

Fig. 5. Effect of nebulin on cross-bridge behavior. (*A* and *B*) Equatorial $I_{1,1}/I_{1,0}$ intensity ratio of resting (*A*) and tetanic (*B*) Ctrl and Neb cKO muscles. (*C*) Intensity of the 4MLL in resting and tetanized Ctrl and Neb cKO soleus. (*D*) Ratio of tetanized to resting 4MLL intensities as a function of genotype. The numbers represent the group mean. $^{**}P < 0.01$; $^{***}P < 0.001$; $^{****}P < 0.0001$.

soleus muscle has been found to be increased (12). Direct measurements on single myofibrils have also shown large force deficits (~50%) in nebulin-free myofibrils (33), indicating that the force deficit is intrinsic to the myofilaments and is not caused by myocyte death. Extensive cell death resulting in fibrosis as a consequence of the absence of nebulin seems unlikely because the collagen area was increased by only ~1% in Neb cKO (*SI Appendix*, Fig. S8), and structural fingerprints such as the 67-nm D-period (axial overlap plus gap repeat) and its higher-order meridionals were not detectable (Fig. 1*C*). Some of the reduced force can be explained by the thin filaments that, on average, are shorter in soleus muscle of Neb cKO mice (12), but estimates indicate that within the physiological working range of soleus muscle this can explain a force deficit of only ~15% (for details, see ref. 12). Thus, other nebulin-based explanations for the force deficit are likely to exist. Our study shows that nebulin deficiency results in an altered troponin arrangement in both passive and active Neb cKO muscle and impairs tropomyosin movement during contraction (Fig. 4), while the expression levels of these regulatory proteins are maintained (*SI Appendix*, Fig. S9 *A–D*). These identified changes in the configuration of thin filament regulatory proteins might influence the activation state of the thin filament and affect the level of force generated for a given level of calcium. Indeed, previous studies on mouse models and nemaline myopathy patients have shown that nebulin deficiency reduces the calcium sensitivity of force generation (30, 34, 35).

How nebulin interacts with tropomyosin and troponin is unknown, but insight can be obtained from an image reconstruction study by Lukoyanova et al. (36), who used F-actin and a short nebulin fragment consisting of four simple nebulin repeats. This work showed multiple nebulin binding sites on the outer domains of each actin subunit, one of which is in close proximity to both the myosin binding site and the blocked state of tropomyosin (36), findings that support the notion that nebulin affects the activation state of the thin filament. Our X-ray study shows alterations in the thin filament helix, as suggested by the unchanged 51 Å and significantly reduced 59 Å spacings (Fig. 3 and *SI Appendix*, Fig. S5), and these structural alterations might also impair troponin and tropomyosin from regulating thin filament activation.

To gain insight into cross-bridge behavior during contraction, we carried out an analysis of the 4MLL. The intensity distribution on the 4MLL reflects the highly ordered helical arrangement of myosin heads around the thick filament backbone and is strongest in relaxed muscle where myosin heads decorate the thick filament at fixed axial intervals (29). Equal 4MLL intensities found in passive muscles of both genotypes (Fig. 5*C*, Resting) suggest that an equal proportion of myosin heads are ordered around the thick filament backbone in both Ctrl and Neb cKO muscles at rest. The 4MLLs did not completely disappear during the tetanus and, interestingly, the ratio of tetanic to passive 4MLL intensities was significantly higher in the Neb cKO (Fig. 5*D*). This finding indicates that in activated muscle, the proportion of the ordered myosin heads that remains around the thick filament backbone is significantly higher in the absence of nebulin. The ratio of layer line intensities also makes it possible to gain insight into the fraction of myosin heads available for force generation during isometric contraction. Considering that the measured X-ray intensity is proportional to the square of the electron density, the measured 4MLL intensity ratio (Fig. 5*D*) indicates that 46% of the myosin heads are interacting with actin in Ctrl muscle, but only 34% in Neb cKO muscle—a 26% reduction. These findings support that the presence of nebulin increases the activation level of the thin filament and that this promotes cross-bridge interaction and force generation.

The ratio of the 1,1 equatorial reflection intensity to that of the 1,0 reflection, $I_{1,1}/I_{1,0}$, reflects the mass distribution between the 1,1 equatorial plane (thin and thick filaments) and the 1,0 plane (thick filaments only), and when myosin heads move from the thin filament to the thick filament, the ratio falls (22). The reduced $I_{1,1}/I_{1,0}$ ratio that was found in nebulin-deficient passive muscle relative to Ctrl (Fig. 5*A*) suggests that more heads are near the thick filament backbone, which is at odds with the 4MLL that reveals no difference in the passive state (see above). Whether the reduced $I_{1,1}/I_{1,0}$ ratio can be explained by the lacking nebulin mass around the thin filament can be assessed as follows. The mass per 40-nm thin filament is ~938 kDa [14 actin monomers × 43 kDa, two troponin–tropomyosin complexes (280 kDa), and two nebulin super repeats (56 kDa)], and deleting nebulin results in a 6.0% decrease. The mass per 40-nm thick filament is ~3,281 kDa (there are ~300 myosin molecules per 1,600-nm long thick filament, each with a mass of 500 kDa). Lastly, in the 1,1 equatorial plane, there are two thin filaments per thick filament (22). Hence, nebulin deficiency is expected to lower the mass of the 1,1 plane by 2.2% and the $I_{1,1}$ by 4.6%. This is much less than the reduction that was found. An alternative explanation for the reduced $I_{1,1}/I_{1,0}$ ratio in passive muscle is that by lowering the stiffness of the thin filament, nebulin deficiency increases the disorder of the thin filament (lateral displacement) and this lowers the $I_{1,1}/I_{1,0}$ ratio, as suggested by both modeling studies (37) and experimental studies on rabbit skeletal muscle fibers that underwent temperature jumps (38).

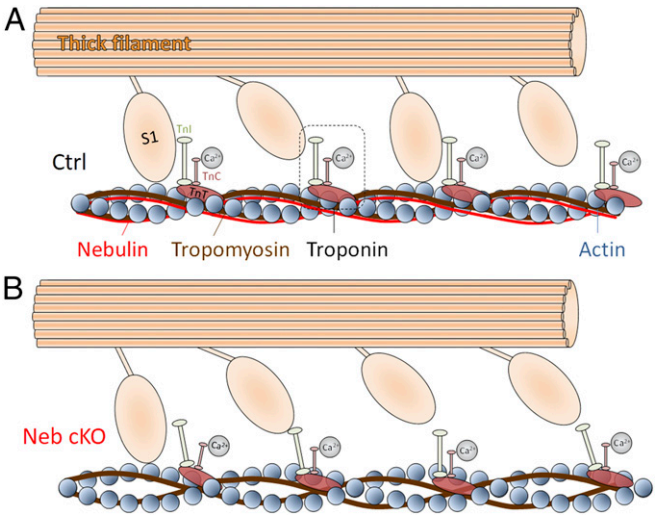

Fig. 6. Nebulin modulates force generation in skeletal muscle. (*A*) Ctrl muscle schematically showing nebulin and regulatory proteins (troponin and tropomyosin) on the thin filament. (*B*) Nebulin deficiency causes impaired tropomyosin/troponin movement, thereby interfering with cross-bridge formation and reducing the tetanic force. See text for details.

It is interesting to reflect on the absence of nebulin in cardiac muscle. In a healthy heart, all myocytes are activated and force can be tuned from a submaximal level (which is the baseline state) to much higher levels, utilizing multiple cardiac-specific post-translational modifications (e.g., as occurs during the fight-or-flight response). To attain such adaptability, it might not be desirable to have nebulin because it would result in a baseline force that is already high and does not have much room to be "tuned up". In skeletal muscle, in contrast, nebulin stiffens thin filaments by directly stabilizing its actin subunits, which is essential for the high levels of thin filament activation that gives rise to the high speeds and force levels that characterizes skeletal muscle, with tunability provided by motor unit recruitment. Muscles deficient in nebulin have greatly increased thin filament extensibility, and this impacts thin filament helix geometry. The twisted thin filament helix alters the configuration of the troponin complex and hinders the movement of tropomyosin, leading to reduced cross-bridge formation and low forces (Fig. 6). The reduced force generated by muscles in nemaline myopathy patients is likely to be the result of the reduced thin filament stiffness that reduces the force-generating cross-bridge population by depressing the thin filament activation level.

Materials and Methods

Altogether, 103 mice (average age, 2 mo) were used in the study. Genotype was determined based on tailtip PCR. Nebulin expression was assessed with Western blot analysis using anti-nebulin N-terminal antibody (*SI Appendix*, Fig. S6). Protein levels of tropomyosin (Tm), troponin-C (TnC), troponin-T (TnT), and troponin-I (TnI) as well as MHC isoform expression were also determined. Routine picrosirius red, Gömöri-trichrome stains (*SI Appendix*, Fig. S8) and electron microscopy were performed on fixed soleus cross-sections. All animal experiments were approved by the University of Arizona and the Illinois Institute of Technology Institutional Animal Care and Use Committees and followed the *Guide for the Care and Use of Laboratory Animals* (39).

Intact soleus muscles were electrically stimulated at optimal muscle length in a custom-built test system (Fig. 1*A*). Blebbistatin was used to inhibit muscle contraction and lower tetanic force. Alternatively, the tetanic force was rapidly lowered by adjusting the muscle length (Fig. 2*C*). Sarcomere length was measured on fixed soleus fiber bundles using a CCD camera (*SI Appendix*, Fig. S7*B*). X-ray diffraction images were recorded using a high-flux 12 keV X-ray beam provided by Beamline 18 at the Advanced Photon Source (Argonne National Laboratory). Individual image frames were summed to be equivalent to at least 0.375 s exposure. The MUSICO computational platform (27) was used to simulate isometric force development and instantaneous muscle stiffness.

Descriptive statistical results are shown as mean ± SD unless stated otherwise. Differences between groups were considered to be statistically significant at a probability value of $P < 0.05$. Symbols used in statistical tests and on figures include ns, $P \geq 0.05$; *$P < 0.05$; **$P < 0.01$; ***$P < 0.001$; and ****$P < 0.0001$. Detailed statistical evaluation is provided in *SI Appendix*, Table S1. Further details are in *SI Appendix, Supplemental Methods*.

ACKNOWLEDGMENTS. This research was supported by Grants R01AR053897 and R01AR073179 from the NIH/National Institute of Arthritis and Musculoskeletal and Skin Diseases and used resources of the Advanced Photon Source, operated under Department of Energy Contract DE-AC02-06CH11357 and supported by Grant 9 P41 GM103622 from the NIH/National Institute of General Medical Sciences (NIGMS). Use of the Pilatus 3 1M detector was provided by Grant 1S10OD018090-01 from the NIH/NIGMS. H.L.G. is the Allan and Alfie Norville Endowed Chair for Heart Disease in Women Research.

1. Labeit S, et al. (1991) Evidence that nebulin is a protein-ruler in muscle thin filaments. *FEBS Lett* 282:313–316.
2. Labeit S, Kolmerer B (1995) The complete primary structure of human nebulin and its correlation to muscle structure. *J Mol Biol* 248:308–315.
3. Pappas CT, Bliss KT, Zieseniss A, Gregorio CC (2011) The nebulin family: An actin support group. *Trends Cell Biol* 21:29–37.
4. Wang K, Wright J (1988) Architecture of the sarcomere matrix of skeletal muscle: Immunoelectron microscopic evidence that suggests a set of parallel inextensible nebulin filaments anchored at the Z line. *J Cell Biol* 107:2199–2212.
5. Wright J, Huang QQ, Wang K (1993) Nebulin is a full-length template of actin filaments in the skeletal muscle sarcomere: An immunoelectron microscopic study of its orientation and span with site-specific monoclonal antibodies. *J Muscle Res Cell Motil* 14:476–483.
6. Jin JP, Wang K (1991) Nebulin as a giant actin-binding template protein in skeletal muscle sarcomere. Interaction of actin and cloned human nebulin fragments. *FEBS Lett* 281:93–96.
7. Kruger M, Wright J, Wang K (1991) Nebulin as a length regulator of thin filaments of vertebrate skeletal muscles: Correlation of thin filament length, nebulin size, and epitope profile. *J Cell Biol* 115:97–107.
8. Trinick J (1992) Understanding the functions of titin and nebulin. *FEBS Lett* 307:44–48.
9. Squire JM, Knupp C (2005) X-ray diffraction studies of muscle and the crossbridge cycle. *Adv Protein Chem* 71:195–255.
10. Lehtokari VL, et al. (2011) Nemaline myopathy caused by mutations in the nebulin gene may present as a distal myopathy. *Neuromuscul Disord* 21:556–562.
11. Ochala J, et al. (2011) Disrupted myosin cross-bridge cycling kinetics triggers muscle weakness in nebulin-related myopathy. *FASEB J* 25:1903–1913.
12. Li F, et al. (2015) Nebulin deficiency in adult muscle causes sarcomere defects and muscle-type-dependent changes in trophicity: Novel insights in nemaline myopathy. *Hum Mol Genet* 24:5219–5233.
13. Ottenheijm CA, et al. (2010) Altered myofilament function depresses force generation in patients with nebulin-based nemaline myopathy (NEM2). *J Struct Biol* 170: 334–343.
14. Elliott GF, Lowy J, Millman BM (1965) X-ray diffraction from living striated muscle during contraction. *Nature* 206:1357–1358.
15. Huxley HE, Stewart A, Sosa H, Irving T (1994) X-ray diffraction measurements of the extensibility of actin and myosin filaments in contracting muscle. *Biophys J* 67: 2411–2421.
16. Wakabayashi K, et al. (1994) X-ray diffraction evidence for the extensibility of actin and myosin filaments during muscle contraction. *Biophys J* 67:2422–2435.
17. Sugi H, Chaen S (2016) Evidence for the regulation of actin-myosin binding strength by lever arm and subfragment-2 regions of myosin molecule in contracting skinned muscle fibers as revealed by the effect of antibodies. *J Nanomed Nanotechnol* 7:415.
18. Brunello E, et al. (2014) The contributions of filaments and cross-bridges to sarcomere compliance in skeletal muscle. *J Physiol* 592:3881–3899.
19. Wakabayashi K, et al. (1985) Time-resolved x-ray diffraction studies on the intensity changes of the 5.9 and 5.1 nm actin layer lines from frog skeletal muscle during an isometric tetanus using synchrotron radiation. *Biophys J* 47:847–850.
20. Ochala J, Iwamoto H, Larsson L, Yagi N (2010) A myopathy-linked tropomyosin mutation severely alters thin filament conformational changes during activation. *Proc Natl Acad Sci USA* 107:9807–9812.
21. Chan C, et al. (2016) Myopathy-inducing mutation H40Y in ACTA1 hampers actin filament structure and function. *Biochim Biophys Acta* 1862:1453–1458.
22. Millman BM (1998) The filament lattice of striated muscle. *Physiol Rev* 78:359–391.
23. Brenner B, Yu LC (1985) Equatorial X-ray diffraction from single skinned rabbit psoas fibers at various degrees of activation. Changes in intensities and lattice spacing. *Biophys J* 48:829–834.
24. Malinchik S, Xu S, Yu LC (1997) Temperature-induced structural changes in the myosin thick filament of skinned rabbit psoas muscle. *Biophys J* 73:2304–2312.
25. Takezawa Y, Sugimoto Y, Wakabayashi K (1998) Extensibility of the actin and myosin filaments in various states of skeletal muscle as studied by X-ray diffraction. *Adv Exp Med Biol* 453:309–316; discussion 317.
26. Linari M, et al. (2015) Force generation by skeletal muscle is controlled by mechanosensing in myosin filaments. *Nature* 528:276–279.
27. Mijailovich SM, et al. (2016) Three-dimensional stochastic model of actin-myosin binding in the sarcomere lattice. *J Gen Physiol* 148:459–488.
28. Maéda Y, Popp D, Stewart AA (1992) Time-resolved X-ray diffraction study of the troponin-associated reflexions from the frog muscle. *Biophys J* 63:815–822.
29. Irving T, et al. (2011) Thick-filament strain and interfilament spacing in passive muscle: Effect of titin-based passive tension. *Biophys J* 100:1499–1508.
30. Witt CC, et al. (2006) Nebulin regulates thin filament length, contractility, and Z-disk structure in vivo. *EMBO J* 25:3843–3855.
31. Kojima H, Ishijima A, Yanagida T (1994) Direct measurement of stiffness of single actin filaments with and without tropomyosin by in vitro nanomanipulation. *Proc Natl Acad Sci USA* 91:12962–12966.
32. Isambert H, et al. (1995) Flexibility of actin filaments derived from thermal fluctuations. Effect of bound nucleotide, phalloidin, and muscle regulatory proteins. *J Biol Chem* 270:11437–11444.
33. Ottenheijm CA, et al. (2013) Deleting exon 55 from the nebulin gene induces severe muscle weakness in a mouse model for nemaline myopathy. *Brain* 136:1718–1731.
34. Chandra M, et al. (2009) Nebulin alters cross-bridge cycling kinetics and increases thin filament activation: A novel mechanism for increasing tension and reducing tension cost. *J Biol Chem* 284:30889–30896.
35. Ottenheijm CA, et al. (2009) Thin filament length dysregulation contributes to muscle weakness in nemaline myopathy patients with nebulin deficiency. *Hum Mol Genet* 18: 2359–2369.
36. Lukoyanova N, et al. (2002) Each actin subunit has three nebulin binding sites: Implications for steric blocking. *Curr Biol* 12:383–388.
37. Malinchik S, Yu LC (1995) Analysis of equatorial x-ray diffraction patterns from muscle fibers: Factors that affect the intensities. *Biophys J* 68:2023–2031.
38. Bershitsky SY, et al. (2010) Myosin heads contribute to the maintenance of filament order in relaxed rabbit muscle. *Biophys J* 99:1827–1834.
39. National Research Council (2011) *Guide for the Care and Use of Laboratory Animals* (National Academies Press, Washington, DC), 8th Ed.